Title	Fundamental Studies on Electron Beam Welding of Heat-resistant Superalloys for Nuclear Plants (Report II) : Correlation between Susceptibility to Weld Cracking and Characteristics in Hot Ductility and Trans-Varestraint Test
Author(s)	Arata, Yoshiaki; Terai, Kiyohide; Nagai, Hiroyoshi et al.
Citation	Transactions of JWRI. 1977, 6(1), p. 69-79
Version Type	VoR
URL	https://doi.org/10.18910/3947
rights	
Note	

Fundamental Studies on Electron Beam Welding of Heat-resistant Superalloys for Nuclear Plants (Report II)[†]

—Correlation between Susceptibility to Weld Cracking and Characteristics in Hot Ductility and Trans-Varestraint Test—

Yoshiaki ARATA*, Kiyohide TERAI**, Hiroyoshi NAGAI**, Shigeki SHIMIZU** and Toshiichi AOTA**

Abstract

In this report, it has been made clear that such criteria well correlate with q_{cr} in the electron beam welding of the heat-resistant superalloys for the nuclear plants as ΔT_B and $_BT_R$ in the hot ductility test and $vT_{R \cdot 5\%}$ in the Trans-Varestraint test and that these tests can be effectively applied to evaluate the susceptibility to microcracking in the electron beam welding. Above-mentioned technical symbols are given meanings in this report.

1. Introduction

In the previous report[1], the effect of electron beam welding conditions on some characteristics of the weld bead, that is, weld profile and weld defects were systematically studied. Two kinds of weld defects, porosity and microcrack (hot crack) herein occurred. As far as it concerns with the microcrack, it has been clarified that microcracking correlates with the weld heat input and that the susceptibility of superalloys to microcracking can be evaluated in terms of the critical heat input to avoid microcrack.

It is of great importance in the prevention of microcrack and the further development of new material to make clear its characteristics and establish the effective criteria for evaluation of the sensitivity to it.

In this report, the respective correlation is investigated on the heat-resistant superalloys for nuclear plants between the sensitivity to microcracking in electron beam welding, the hot ductility characteristics on the simulated weld thermal cycle and the results in Trans-Varestraint and Varestraint test conventionally used for the sensitivity to hot cracking. Such testing methods as hot ductility, Trans-Varestraint and Varestraint test can be considered to be effective ones in the evaluation of sensitivity to microcracking.

2. Material used

Such superalloys as Hastelloy type, Inconel type and Incoloy type and austenitic stainless steel for comparison were used. These chemical composition, mechanical properties etc. are shown in **Table 1**.

Table 1 Chemical Composition and Mechanical Properties of Superalloys used

Material	Mark	Thickness (mm)	Melting Process	Final Heat Treatment	Grain Size (ASTM)	0.2%PS (kg/mm²)	T.S (kg/mm²)	El. (%)	R of A (%)	C	Si	Mn	P	S	Ni	Cr	Co	Mo	W	Nb·Ta	Al	Ti	B	Zr	Ce	Fe	O	N Sol.	N Insol.	N Total
Hastelloy X	HAEN	20	AE	1120°C×18Min W.Q.	1~4	30.4	71.1	59.0	65.0	0.066	0.48	0.88	0.016	<0.002	Bal.	21.36	1.77	9.05	0.45		0.07	0.15	0.002			19.09	3	405	42	447
	HAEM		AE	1150°C×50Min W.Q.	5~6	38.7	75.0	47.6	—	0.068	0.37	0.59	0.012	<0.002		20.74	1.03	8.70	0.50	—	0.21	0.02	0.0001	—	—	18.23	2	248	20	268
	HVEN		VE	1120°C×18Min W.Q.	1~6	34.3	73.8	49.3	56.9	0.084	0.17	0.84	0.001	<0.002		20.70	1.59	9.20	0.55		0.02	0.19	0.002			18.53	5	306	16	322
	HVERN		VE	1170°C×30Min A.C.	1~4	32.4	74.0	54.3	52.2	0.065	0.35	0.72	0.001	<0.002		21.40	1.45	8.93	0.51	0.05	0.05	0.06	0.002	0.009	<0.005	19.08	4	121	22	143
Inconel 625	Inl 625AE	20	AE	1000°C×1Hr W.Q.	6	45.5	90.1	46.8	—	0.053	0.28	0.24	0.003	<0.002	Bal.	22.09	0.06	8.81	0.69	3.53	0.24	0.13	—	—	—	2.54	3	44	211	255
Inconel 617	Inl 617V		V	1177°C W.Q.	3~4	30.0	74.6	70.0	57.0	0.066	0.17	0.02	0.004	<0.002		21.24	12.60	9.00	—	—	0.93	0.52	—	—	—	1.45	4	244	180	424
Incoloy 800	Iny 800V		V	1100°C×15Hr W.Q.	2.5	22.1	58.2	52.0	72.1	0.056	0.07	0.77	0.010	0.002	32.13	21.21	0.50	0.18	—	—	0.51	0.59	—	—	—	Bal.	6	32	93	125
Incoloy 807	Iny 807A		A	1230°C×3Hr W.Q.	1	25.7	64.1	52.2	60.3	0.057	0.50	0.70	0.002	0.002	40.10	20.58	8.28	0.20	4.85	0.99	0.47	0.24	—	—	—	Bal.	7	68	144	212
SUS 316	S 316		A	1100°C×13Min W.Q.	3~5	—	60.3	61.4	—	0.045	0.79	1.26	0.028	0.004	11.51	17.52	—	2.58	—	—	—	—	—	—	—		13	257	32	289

‡ AE : Air Melting followed by Electroslag Remelting. VE : Vacuum Induction Melting followed by Electroslag Remelting.
V : Vacuum Induction Melting. A : Air Melting

Hastelloy type superalloys are below mentioned in such symbols as HAEN, HAEM, HVEN and HVERN.

3. Experimental Instrument and Procedure

3.1 Hot ductility test

Weld thermal cycle simulator, which works under the high frequency heating system and electro-hydraulic one was used. Its Max. load and Max. tensile rate are 5 ton and 30 mm/sec respectively.

Simulating the weld thermal cycle on the hot ductility test specimen, rapid tensile test was carried out under the controlled tensile rate of 30 mm/sec at the various temperature both on heating and on cooling. Hot ductility test specimen and simulated weld thermal cycle are shown in **Fig. 1** and **Fig. 2**, respectively. After
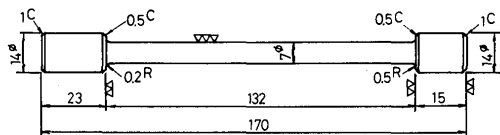
Fig. 1 Hot Ductility Test Specimen
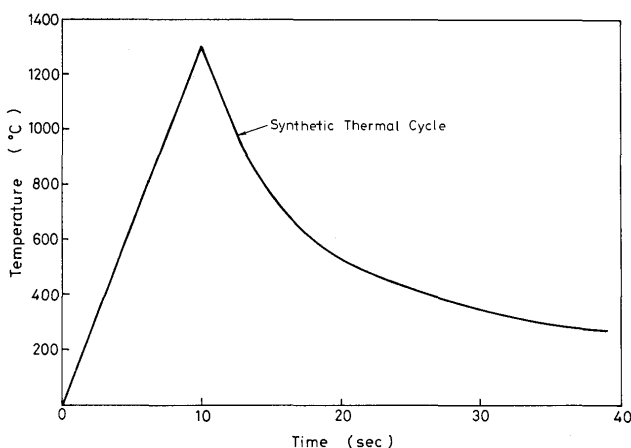
Fig. 2 Simulated Weld Thermal Cycle

the tensile test, rupture load was obtained on the recorded time vs. load diagram and reduction of area was calculated directly from two-direction diameters intersecting at right angle.

3.2 Trans-Varestraint and varestraint test

The essential detail of the Trans-Varestraint testing apparatus is shown in **Fig. 3**. As described in this figure, 5 mm-thick specimen was set on the radiused bending block and TIG arc welding was performed from the starting point A to C on the welding conditions of 100A×8.5V×100 mm/min. Then, as the arc passed the point B apart from A by 30 mm, two hydraulically-actuated yokes attached to the cylinder
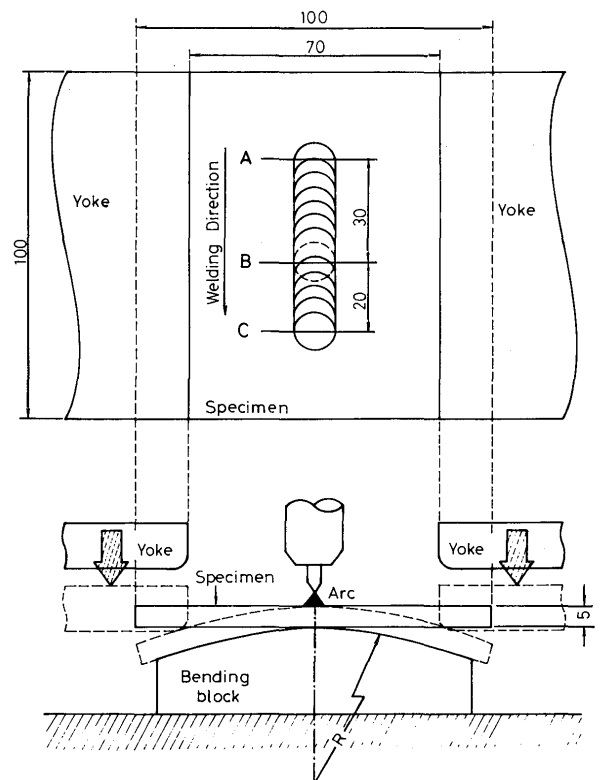

Fig. 3 Schematic Explanation of Trans-Varestraint Test

bent the specimen downward suddenly under the bending speed of 300 mm/sec to conform it to the radius of curvature of the bending block. The arc traveled steadily onward and was subsequently extinguished at the point C apart from B by 20 mm to avoid the crater cracking. Meanwhile, the welding direction in the Varestraint test meets that of Trans-Varestraint test at right angle and bending strain is augmented just as the arc passes the top point of bending block.

The augmented strain ε in the outer fiber of the specimen can be calculated as follows:

$$\varepsilon \doteqdot \frac{t}{2R} \times 100(\%)$$

where; t: specimen thickness, R: radius of the curvature of bending block

Therefore, by substituting the bending block with the appropriate radius of the curvature, any desired augmented strain can be applied to the welds at the predetermined instant during welding.

To measure the weld thermal cycle at the centerline of the weld bead, fine wire thermocouple with the diameter of 0.25 mm, W.5%Re-W.26%Re, was plunged into the molten weld puddle directly behind the arc along the centerline of the weld bead during TIG arc welding. The output of the thermocouple was recorded by means of electromagnetic oscillograph.

After welding, cracks occurred in the welds were observed at the magnification of 80 by the practical microscope.

3.3 Measurement of melting temperature

Differential temperature analysing apparatus was used to measure the melting temperature of the superalloys. Solid bar of every superalloy was inserted into the alumina container, heated up to 1500°C to be melted and cooled down to 1260°C under the constant cooling rate of 5°C/min. Liquidus temperature T_L and solidus temperature T_s were respectively obtained from the slight temperature change resulted from the latent heat of solidification.

4. Experimental Result and Discussion

4.1 Melting temperature of superalloys

Table 2 shows the temperature of solidification start T_L and that of solidification finish T_s, which might be considered to nearly correspond to the temperature of melt finish and that of melt start respectively.

Table 2 Melting Temperature measured

Material	Mark	Melting Temperature (°C)		
		T_L	T_s	ΔT ($= T_L - T_s$)
Hastelloy X	HAEN	1337	1316	21
	HAEM	1367	1345	22
	HVEN	1347	1329	18
	HVERN	1352	1334	18
Inconel 625	Inl 625AE	1321	1305	16
Inconel 617	Inl617V	1375	1349	26
Incoloy 800	Iny800V	1417	1382	35
Incoloy 807	Iny807A	1394	1366	28
SUS 316	S 316	1417	1396	21

Notes : T_L : Liquidus Temperature
T_s : Solidus Temperature

As shown in Table 2, these temperatures depend on the heat even if the superalloys are of the same material just as Hastelloy X. Fe-base superalloys are generally higher than Ni-base superalloys in these temperatures. Meanwhile, solidification temperature range of Ni-base superalloys is smaller than that of Fe-base superalloys.

4.2 Hot ductility characteristics on heating and on cooling

4.2.1 Hot ductility on heating

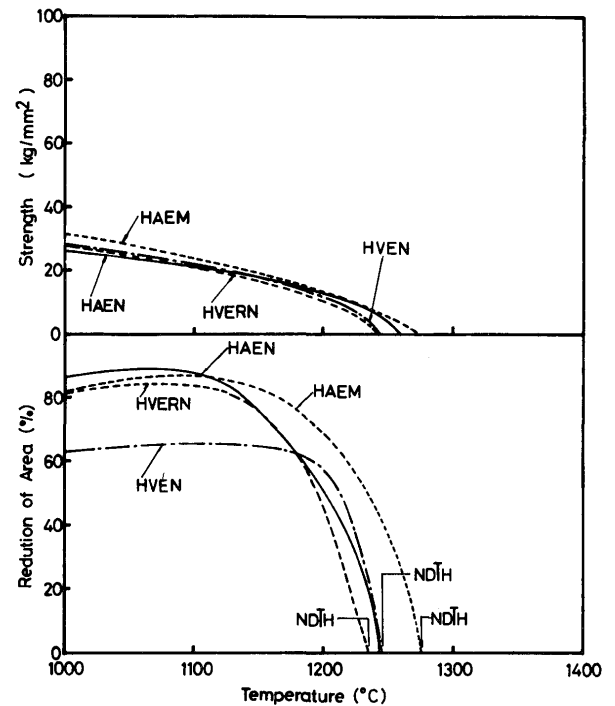Figs. 4 to 6 show the hot ductility test results on

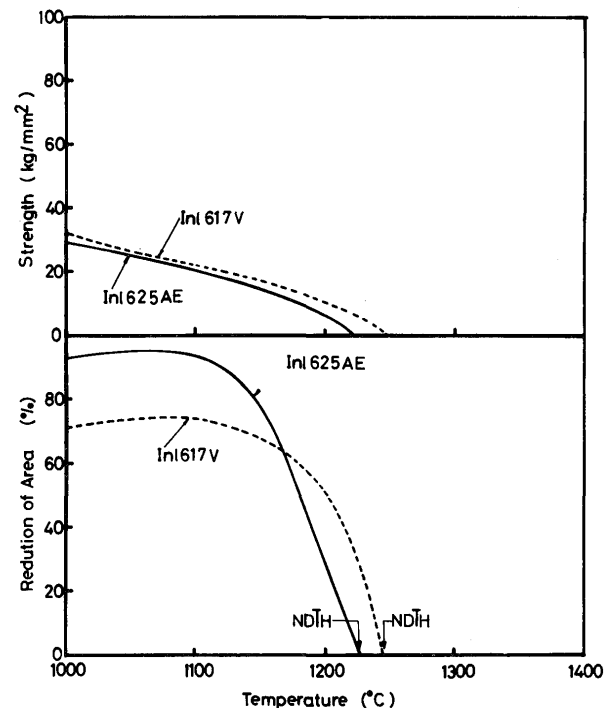Fig. 4 Effect of Temperature on Hot Ductility Characteristics on Heating (Hastelloy X)

Fig. 5 Effect of Temperature on Hot Ductility Characteristics on Heating (Inconel-type Superalloys)

heating. As described in these figures, it is fully recognized without distinction of the superalloys that reduction of area decreases drastically to zero at the certain temperature as seen in the brittle fracture. It might be considered that the hot ductility of superalloys can be evaluated in terms of this nil ductility temperature on heating $_{ND}T_H$. On the assumption that
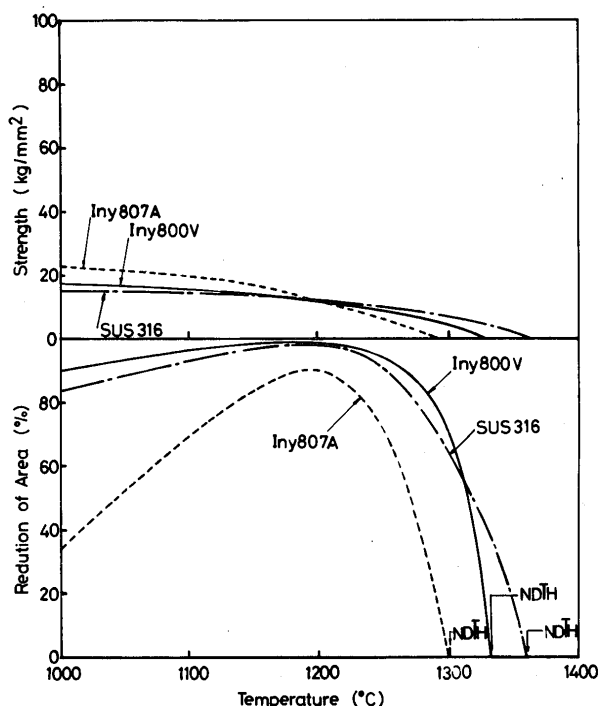
Fig. 6 Effect of Temperature on Hot Ductility Characteristics on Heating (Fe-base Superalloys)

high $_{ND}T_H$ essentially means superior hot ductility, HAEM is most superior of the Ni-base superalloys and is followed by Inconel 617, (HAEN, HVEN), HVERN and Inconel 625 in this order. Meanwhile, SUS316 is the best one of the Fe-base superalloys and is followed by Incoloy 800 and Incoloy 807 in this order.

In any case, rupture stress gradually decreases with the elevation of temperature and becomes very small at the nil ductility temperature on heating $_{ND}T_H$.

4.2.2 Hot ductility on cooling

The effect of peak temperature on the hot ductility on cooling has already been reported[2] and it has been recognized that hot ductility on cooling generally decreases with the elevation of peak temperature. Therefore, peak temperature must be attached full considerations to investigate the correlation between the susceptibility to microcracking in electron beam welding and the hot ductility characteristics on cooling.

(1) Proper Peak Temperature

As described in the previous report[1], the microcrack in the electron beam welds of the superalloys occurred at the weld boundary zone. Therefore, to evaluate the superalloys in the susceptibility to microcracking peak temperature should be established at the temperature where the weld boundary zone is heated in electron beam welding. However, it is really next to impossible to measure it.

The effect of peak temperature on the scanning electron micrograph of the cross-section was system-

atically studied with the peak temperature changed from $_{ND}T_H$ to T_s approximately, simulating the thermal cycle shown in Fig. 1. **Photo. 1** shows the typical
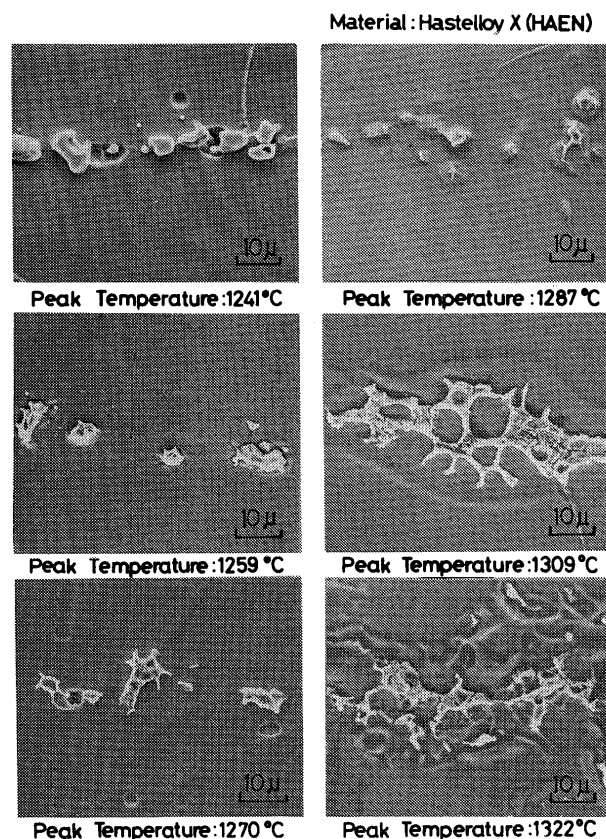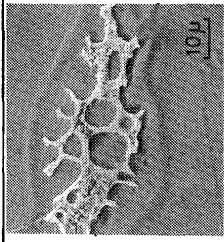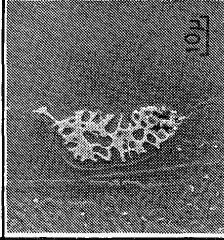
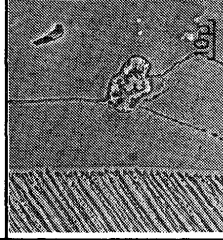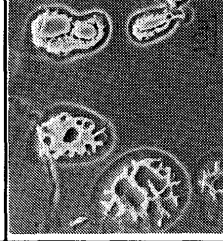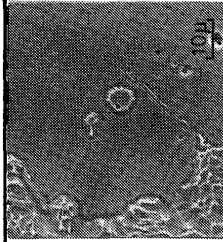**Material : Hastelloy X (HAEN)**
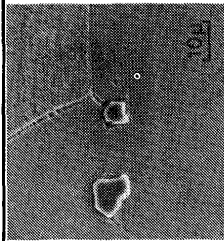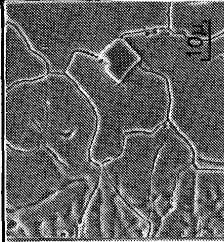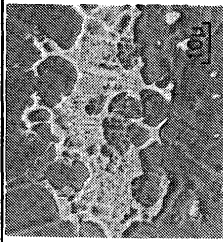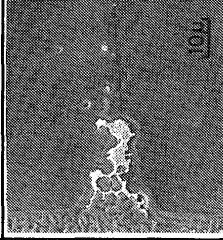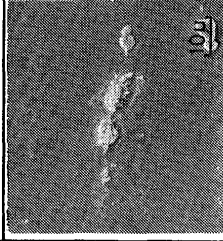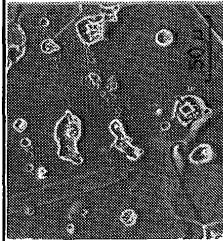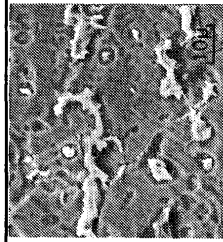
Photo.1 Typical Effect of Peak Temperature on Scanning Electron Micrograph of Hot Ductility Test Specimen (Hastelloy X, HAEN)

example. The peak temperature, to which the heat affected zone adjacent to the weld boundary is heated in electron beam welding, was estimated in view of the precipitates' condition, comparing the scanning electron micrograph of the hot ductility test specimen with that of the heat affected zone. **Table 3** shows the scanning electron micrograph of the hot ductility test specimen similar to that of the heat affected zone of electron beam welds. The proper peak temperature is herein noted.

As described in Table 3, HAEN, HAEM, HVEN, Inconel 617 and Incoloy 807 accompanies the full melting of the precipitates. Thereby, skelton-like structure can be clearly observed except for Incoloy 807. HVERN accompanies many concavities which might have resulted from the exfoliation of the fine precipitates. This exfoliation is considered to have been caused by polishing and etching. In Inconel 625, only partial melting of the precipitates is observed. Meanwhile, Incoloy 800 and SUS316 accompany no change in the precipitates' condition.

Table 3 Scanning Electron Micrograph of Hot Ductility Test Specimen tested under Proper Peak Temperature

Metallurgy on the precipitates' morphology and microcracking in the heat affected zone shall be discussed in the following report.

(2) Hot Ductility

Hot ductility test results on cooling are shown in **Figs. 7 to 9**. As recognized in these figures, reduction of area decreases to zero at the certain temperature. Hot ductility on cooling is generally poor as compared
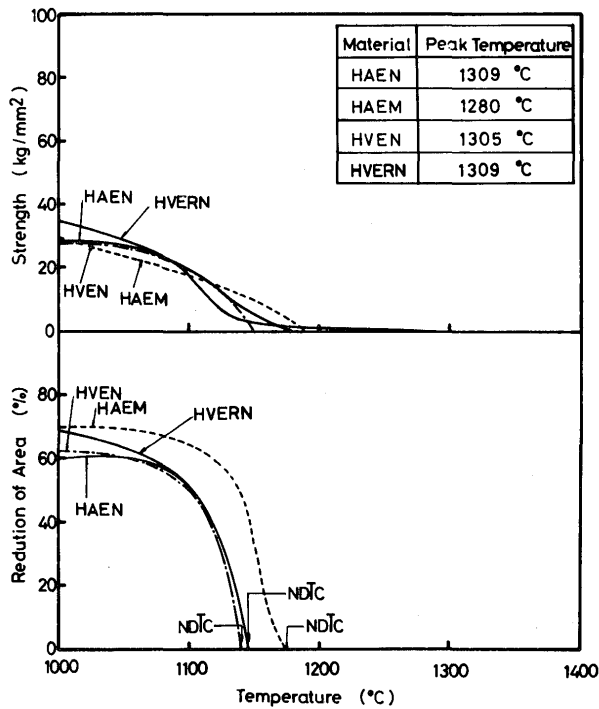

Material	Peak Temperature
HAEN	1309 °C
HAEM	1280 °C
HVEN	1305 °C
HVERN	1309 °C

Fig. 7 Effect of Temperature on Hot Ductility Characteristics on Cooling (Hastelloy X)

Material	Peak Temperature
Inl625AE	1257 °C
Inl617V	1324 °C
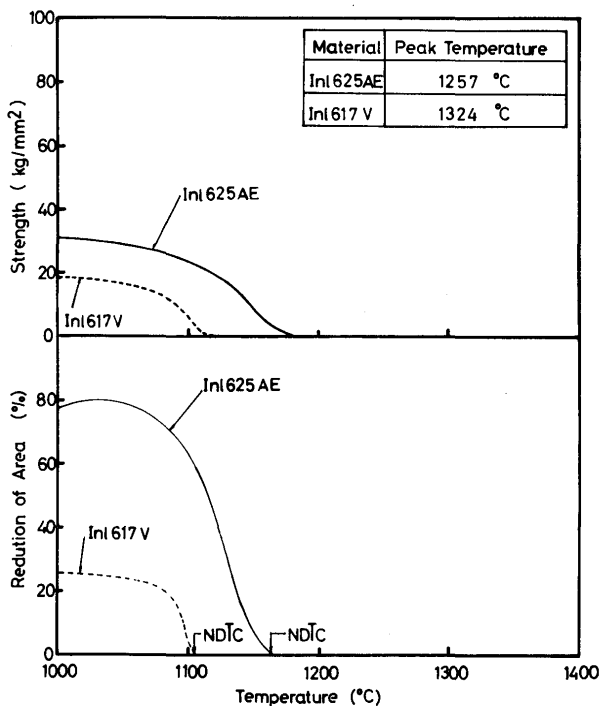
Fig. 8 Effect of Temperature on Hot Ductility Characteristics on Cooling (Inconel-type Superalloys)

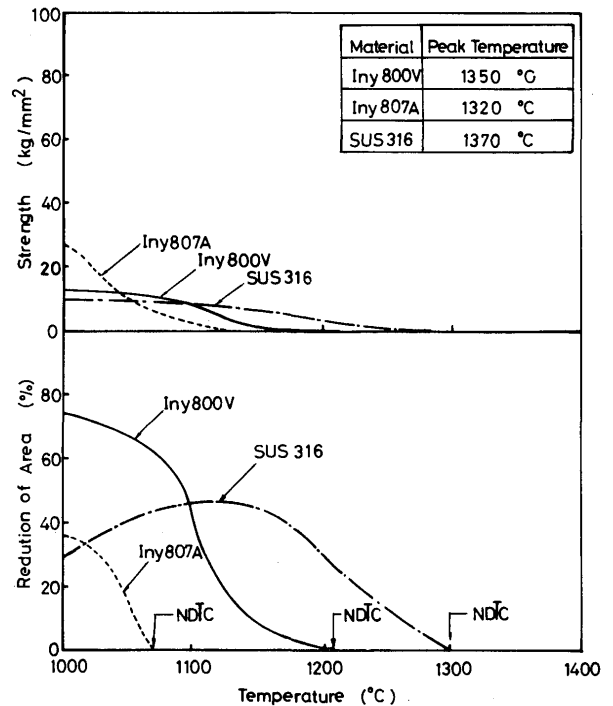| Material	Peak Temperature
Iny800V	1350 °C
Iny807A	1320 °C
SUS316	1370 °C

Fig. 9 Effect of Temperature on Hot Ductility Characteristics on Cooling (Fe-base Supperalloys)

with that on heating. It might be considered that the hot ductility of superalloys can be evaluated in terms of this nil ductility temperature on cooling $_{ND}T_C$. On the assumption that high $_{ND}T_C$ essentially means superior hot ductility, HAEM is most superior of the Ni-base superalloys and is followed by Inconel 625, HVERN, HAEN, HVEN and Inconel 617 in this order. Meanwhile, SUS316 is the best one of the Fe-base superalloys and is followed by Incoloy 800 and Incoloy 807 in this order.

In any case, rupture stress gradually decreases with the elevation of temperature and becomes very small at the nil ductility temperature on cooling $_{ND}T_C$.

4.3 Correlation between susceptibility to microcracking and criteria obtained in hot ductility

As described in the previous report[1], microcrack occurred in the electron beam welds by the bead-on-plate welding method. The clear dependence was herein recognized between this microcrack and weld heat input. The susceptibility of the superalloys to microcracking could be evaluated in terms of the critical heat input to avoid microcrack q_{cr} under which microcrack never occurred.

The criteria related to the susceptibility to microcracking obtained from the hot ductility characteristics and melting temperatures are below explained and the properties of these criteria are shown in **Fig. 10**.
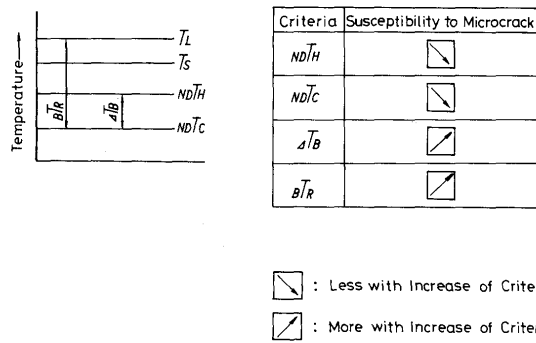
Criteria	Susceptibility to Microcrack
$_{ND}T_H$	◣
$_{ND}T_C$	◣
$_ΔT_B$	◳
$_BT_R$	◳

◣ : Less with Increase of Criteria

◳ : More with Increase of Criteria

Fig. 10 General Effect of Criteria obtained in Hot Ductility Test on Susceptibility to Microcrack

$_{ND}T_H$: temperature at which reduction of area decreases to zero on heating, less susceptible to micracracking with increase of this value

$_{ND}T_C$: temperature at which reduction of area decreases to zero on cooling, less susceptible to microcrack with increase of this value

$ΔT_B$: temperature range between $_{ND}T_H$ and $_{ND}T_C$, more susceptible to microcrack with increase of this value

$_BT_R$*: brittle temperature range between temperature of solidification start T_L (temperature of melt finish) and $_{ND}T_C$, more susceptible to microcrack with increase of this value

Table 4 shows these criteria of the superalloys

Table 4 Criteria obtained in Hot Ductility Test

Material	Mark	$_{ND}T_H$ (°C)	$_{ND}T_C$ (°C)	$ΔT_B$ ($_{ND}T_H$-$_{ND}T_C$) (°C)	$_BT_R$ (T_L-$_{ND}T_C$) (°C)	q_{cr} (joule/cm)
Hastelloy X	HAEN	1244	1142	102	195	1406
	HAEM	1275	1175	100	192	2143
	HVEN	1244	1136	108	211	1286
	HVERN	1235	1143	92	191	<750
Inconel625	In625AE	1225	1163	62	158	>5080
Inconel 617	In617V	1245	1110	135	265	<750
Incoloy 800	Iny800V	1330	1210	120	207	1286
Incoloy807	Iny807A	1300	1070	230	324	1200
SUS 316	S316	1360	1300	60	117	>5080

Notes; $_{ND}T_H$: Nil Ductility Temperature Heating
$_{ND}T_C$: Nil Ductility Temperature Cooling
T_L : Liquidus Temperature
q_{cr} : Critical Heat input to Avoid Microcrack

collectively in comparison with q_{cr}. As shown in **Figs. 11** and **12**, $ΔT_B$ and $_BT_R$ correlate very closely with q_{cr} respectively. The superalloys tend to be more susceptible to microcracking with the increase of $ΔT_B$ and $_BT_R$, that is, with the decrease of q_{cr}.
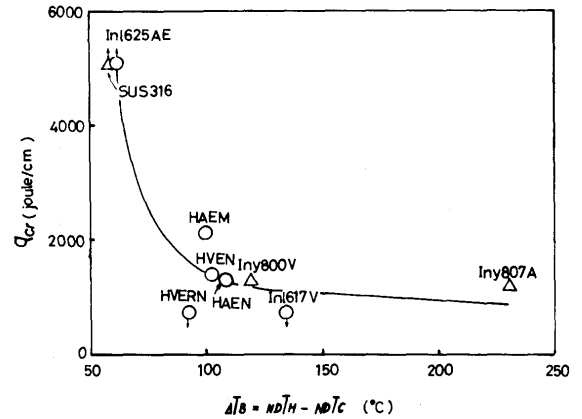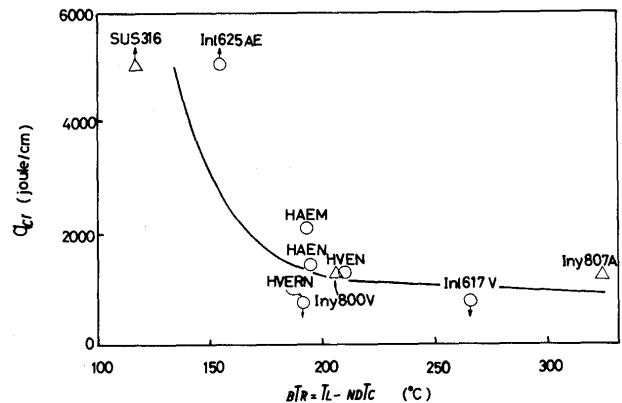

Fig. 11 Correlation between $ΔT_B$ and q_{cr}

Fig. 12 Correlation between $_BT_R$ and q_{cr}

4.4 Trans-Varestraint and varestraint test

4.4.1 Trans-Varestraint test

The Cracks observed by the practical microscope can be grouped into two categories, solidification cracks in the weld metal and liquation cracks in the heat affected zone, as schematically shown in **Fig. 13**. **Photo. 2** shows typical cracks occurred at the instant of the application of augmented strain. Solidification cracks are generally observed between two specific ripple lines and the crack of maximum length usually occurs near the centerline of the weld bead. Meanwhile, liquation cracks also extend from the same ripple line toward the base metal.

* It is proposed in the "generalized theory[3]" by Borland that solidification crack occurs below the lowest temperature where the residual liquidus can heal the cleavage. This temperature is not clear. However, it might be regarded as the liquidus temperature T_L approximately[4]. Therefore, the upper limit of brittle temperature range was herein determined as T_L.
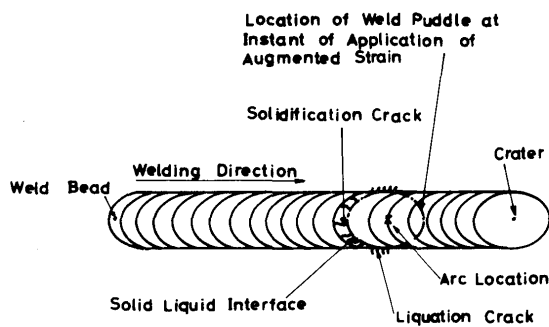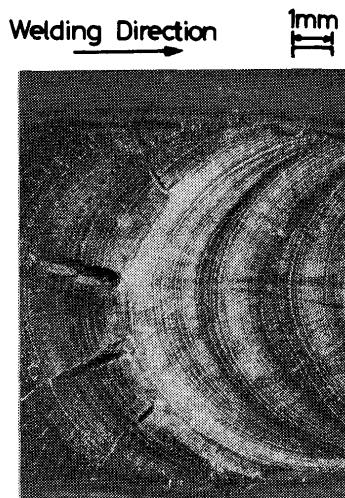
Location of Weld Puddle at
Instant of Application of
Augmented Strain

Solidification Crack

Welding Direction

Weld Bead

Crater

Arc Location

Solid Liquid Interface

Liquation Crack

Fig. 13 Schematic Representation of Cracks observed in Trans-Varestraint Test

Welding Direction   1mm

Welding Conditions :
8.5V-100A-100 mm/min

Material : Inconel 617 (Inl 617V)
Augmented Strain : 2.45%

Photo.2 Typical Cracks observed in Trans-Varestraint Test (Inconel 617)

Hot cracking usually occurs within the certain temperature range just after the solidification where the ductility of the material is essentially very poor. Brittle temperature range in the Trans-Varestraint test is herein defined as $v_B T_R$ or $v T_R$. This $v T_R$ is considered to affect the susceptibility to microcracking.

The magnitude of this $v T_R$ is decided on the temperature vs. augmented strain diagram obtained from the relation between the maximum crack length and the thermal cycle at the centerline of the weld bead[4]. **Figs. 14** and **15** show $v T_R$ of Ni-base and Fe-base superalloys respectively. In these figures, the hatched area represents brittle temperature range of the superalloys. **Table 5** evaluates the superalloys in terms of $v T_{R.5\%}$* which is defined as the brittle temperature range at the augmented strain of 5%. As shown in Table 5, Inconel 617 is most sensitive one to micro-
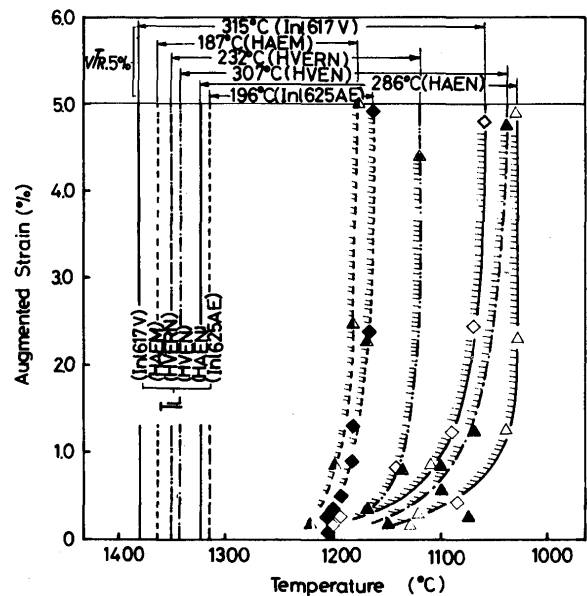

Fig. 14 Brittle Temperature Range of Ni-base Superalloys obtained in Trans-Varestraint Test
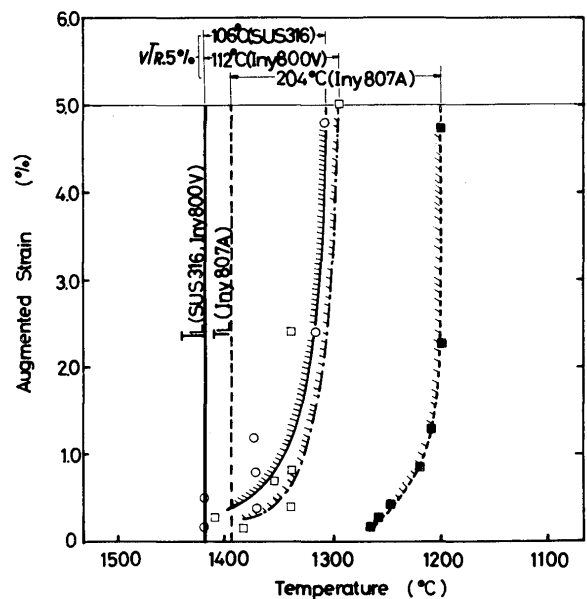

Fig. 15 Brittle Temperature Range of Fe-base Superalloys obtained in Trans-Varestraint Test

cracking of the Ni-base superalloys and followed by HVEN, HAEN, HVERN, Inconel 625 and HAEM in this order. Meanwhile, Incoloy 800 is most sensitive one of the Fe-base superalloys and followed by Incoloy 807 and SUS316 in this order.

4.4.2 Varestraint test

In the Varestraint Test, the specimen is bent longitudinally to the weld bead and the susceptibility to liquation cracking in the heat affected zone can be effectively evaluated.

* $v T_R$ in Trans-Varestraint test depends on the augmented strain. For such a reason, susceptibility to microcracking was evaluated in terms of $v T_{R.5\%}$ defined as the brittle temperature range at the augmented strain of 5 %.

Table 5 Criteria obtained in Trans-Varestraint Test and Varestraint Test

Material	Mark	$V T_{R.5\%}$ in Trans Varestraint Test(°C)	Ll.max(1%) in Varestraint Test(mm)	q_{cr} (joule/cm)	Hot Ductility Test ΔT_B(°C)	Hot Ductility Test $_BT_R$(°C)
Hastelloy X	HAEN	286	0.26	1406	102	195
	HAEM	187	0.42	2143	100	192
	HVEN	307	0.19	1286	108	211
	HVERN	232	0.46	<750	92	191
Inconel 625	Inl 625 AE	196	0.16	>5080	62	158
Inconel 617	Inl 617 V	315	0.55	<750	135	265
Incoloy 800	Iny 800V	112	0.06	1286	120	207
Incoloy 807	Iny 807A	204	0.17	1200	230	324
SUS 316	S 316	106	0.04	>5080	60	114

Notes; $V T_{R.5\%}$: Cracking Temperature Range at Augmented Strain of 5% in Trans-Varestraint Test

Ll.max(1%) : Max. Length of Liquation Crack for 1% Augemented Strain in Varestraint Test

q_{cr} : Critical Heat Input to Avoid Microcrack

ΔT_B : $ND T_H - ND T_C$

$_BT_R$: $T_L - ND T_C$

It is fully recognized by the practical microscope just as in the Trans-Varestraint test that the cracks can be classified into two groups, solidification cracks in the weld metal and liquation cracks in the heat affected zone as shown in **Photo. 3**. Solidification cracks is generally observed between two specific ripple lines and liquation cracks also extend from the same ripple line toward the base metal.

Welding Direction
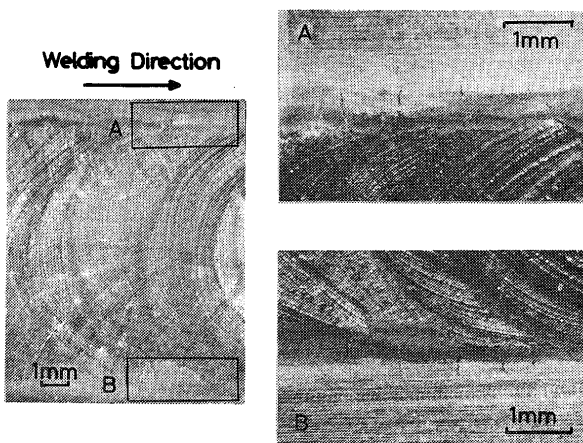
Welding Conditions:
85V-100A-100mm/min
Material: Inconel617 (Iny617V)
Augmented Strain: 1.26%

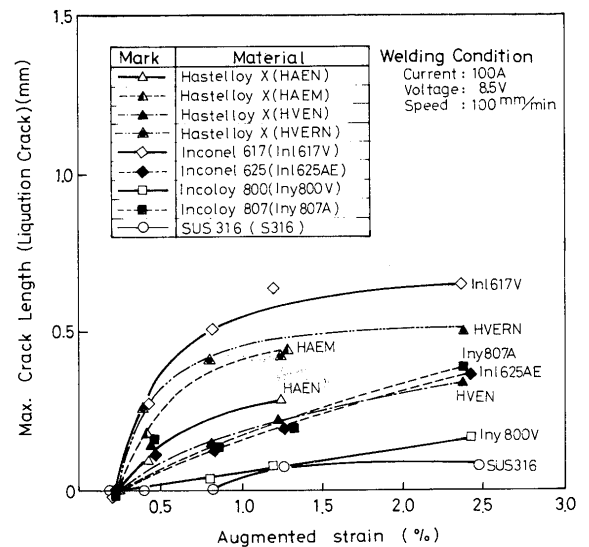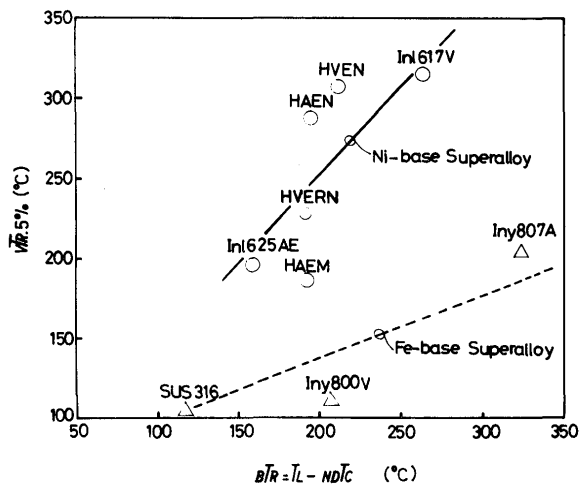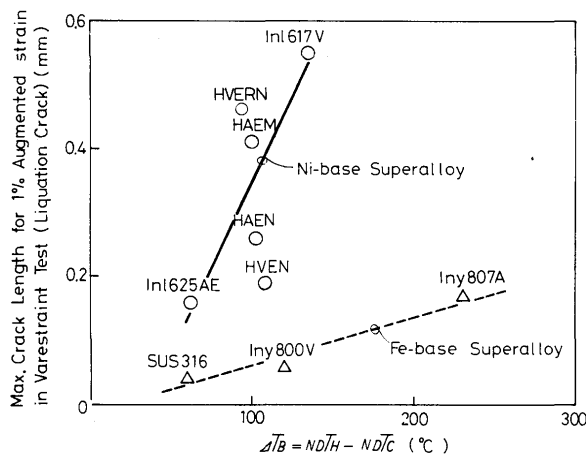**Photo.3** Typical Cracks observed in Varestraint Test (Inconel 617)

Fig. 16 Relation between Augmented Strain and Max. Liquation Crack Length

Fig. 16 shows the relation between the augmented strain and maximum liquation crack length. The minimum augmented strain required to cause cracking is 0.8% and 0.2% approximately for SUS316 and other superalloys respectively. The maximum crack length of Inconel 617, HVERN and SUS316 increases drastically up to the augmented strain of 1% and thereafter comes near to the constant value. While, that of Incoloy 807, Inconel 625, HVEN and Incoloy 800 tends to gradually increase even after the augmented strain exceeds 2.5%. Table 5 evaluates the susceptibility of the superalloys to microcracking in terms of the maximum crack length at the augmented strain of 1%. It is essentially considered that larger maximum crack length means more susceptibility to liquation cracking. From this point of view, Inconel 617 is most sensitive one of the Ni-base superalloys and is followed by HVERN, HAEM, HAEN, HVEN and Inconel 625 in this order. Of the Fe-base superalloys, Incoloy 800 is the most susceptible one and followed by Incoloy 807 and SUS316 in this order.

4.5 Correlation between criteria obtained in Trans-Varestraint and Varastraint and hot ductility test

Criteria related to the susceptibility to microcracking in Trans-Varestraint and Varestraint test, that is, $V T_{R.5\%}$ in Trans-Varestraint test and maximum crack length at the augmented strain of 1% in Varestraint Test correlate with ΔT_B and $_BT_R$ obtained in the hot ductility test, as shown in **Figs. 17** to **20**. As far as it concerns with Hastelloy X, criteria obtained in Trans-Varestraint and Varstraint test depend a little on the heat. It is easily recognized from these
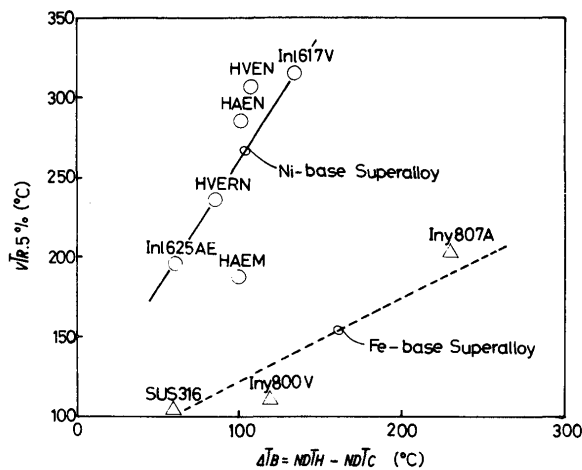
Fig. 17 Correlation between ΔT_B and $_V T_{R.5\%}$
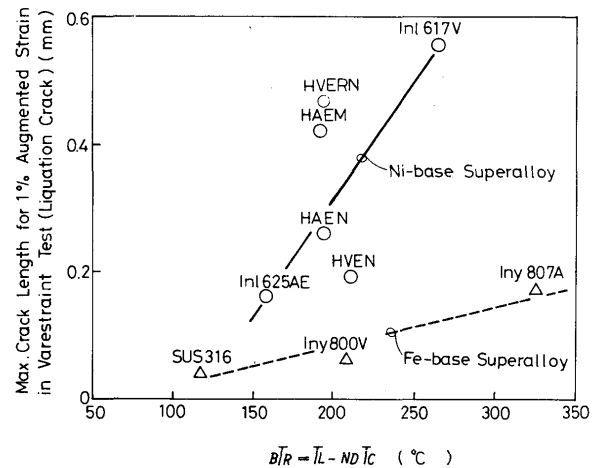
Fig. 20 Correlation between $_B T_R$ and Max. Crack Length in Varestraint Test

figures that Ni-base superalloys are generally more susceptible to microcracking than Fe-base ones, comparing the former superalloys with the latter ones on ΔT_B and $_B T_R$ of the same value.

From the morphological viewpoint of the cracks in the Trans-Varestraint test, Ni-base superalloys accompanies long and greatly opened cracks occurred at the instant of application of the augmented strain as shown in Photo. 2. Thereby, the fiber stress of the specimen is easily released and few cracks occurs between two specific ripple lines. Meanwhile, many a small cracks can be observed between the ripple lines in Fe-base superalloys as shown in **Photo. 4**.

Fig. 18 Correlation between $_B T_R$ and $_V T_{R.5\%}$

Welding Direction   1mm

Welding Conditions :

8.5V-100A-100 mm/min

Material : Incoloy 800 (Iny800V)

Augmented Strain : 2.40 %

Photo.4 Typical Cracks observed in Trans-Varestraint Test (Incoloy 800)

Fig. 19 Correlation between ΔT_B and Max. Crack Length in Varestraint Test

In this report, $_{V}T_{R.5\%}$ obtained from the maximum crack length is used as one of the criteria to evaluate the superalloys in the susceptibility to microcracking notwithstanding the fact that cracking morphology differs in Ni-base and Fe-base superalloys. For such a reason, Ni-base superalloys are considered to be generally more susceptible to microcracking than Fe-base ones in terms of $_{V}T_{R.5\%}$, comparing the former superalloys with the latter ones on ΔT_B and $_{B}T_R$ of the same value. Same tendency was shown in the Varestraint test.

4.6 Correlation between susceptibility to microcracking and criteria obtained in Trans-Varestraint and Varestraint Test

As described in the preceding item, $_{V}T_{R.5\%}$ obtained in Trans-Varestraint test and the maximum crack length at the augmented strain of 1% in Varestraint test are considered to be effective as one of the criteria to evaluate the superalloys in the susceptibility to microcracking.

Table 5 summarizes these criteria in comparison with the critical heat input to avoid microcrack q_{cr}. **Figs. 21 and 22** show the relation between these criteria and
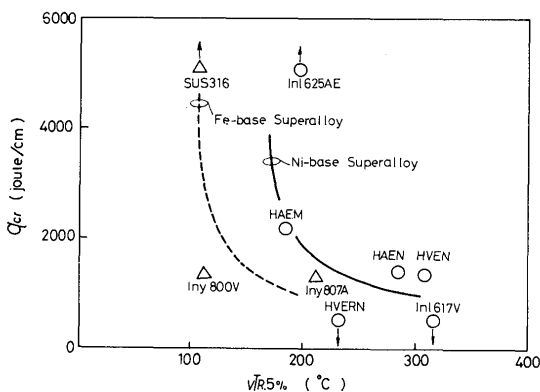

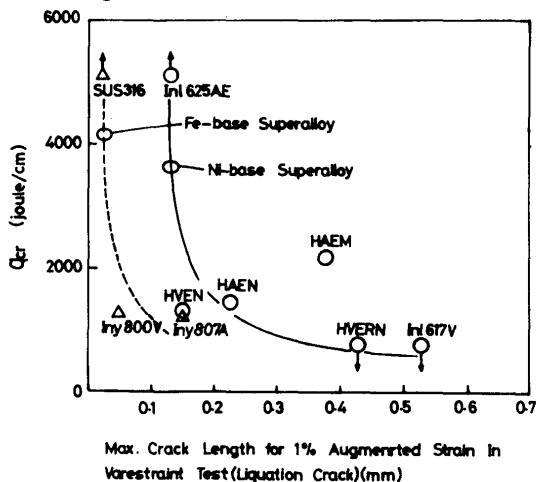**Fig. 21** Correlation between $_{V}T_{R.5\%}$ and q_{cr}

Fig. 22 Correlation between Max. Crack Length in Varestraint Test and q_{cr}

q_{cr} in which clear correlation is recognized.

HVERN deviates from the relation between $_{V}T_{R.5\%}$ and q_{cr} in Fig. 21. However, it does agree closely with the general tendency between maximum length of the liquation crack and q_{cr} in Fig. 22. This might be because most microcracks occurred in the electron beam welds of this material belongs to the liquation cracks.

5. Conclusion

The Correlation was herein investigated between the susceptibility to microcracking in electron beam welding and characteristics of the hot ductility, Trans-Varestraint and Varestraint test. Obtained conclusion may be summarized as follows;

(1) Such criteria obtained in the hot ductility test are employed to evaluate the susceptibility to microcracking as $_{ND}T_H$ (nil ductility temperature on heating), $_{ND}T_C$ (nil ductility temperature on cooling), ΔT_B ($\equiv _{ND}T_H - _{ND}T_C$) and $_{B}T_R$ (brittle temperature range between temperature of solidification start T_L and $_{ND}T_C$). Of these criteria, ΔT_B and $_{B}T_R$ best correlate with the critical heat input to avoid microcrack q_{cr} which is one of the effective criteria to evaluate the susceptibility to it in the electron beam welding.

(2) Such criteria obtained in the Trans-Varestraint and Varestraint test are effective ones to evaluate the susceptibility to microcracking as $_{V}T_{R.5\%}$ (brittle temperature range at the augmented strain of 5% in the Trans-Varestraint test) and maximum crack length at the augmented strain of 1% in the Varestraint test. These criteria well correlate with q_{cr}.

(3) Correlation can be recognized between ΔT_B and $_{B}T_R$ in the hot ductility test, $_{V}T_{R.5\%}$ in the Trans-Varestraint test and maximum crack length at the augmented strain of 1% in the Varestraint test.

References

1) Yoshiaki Arata, Kiyohide Terai, Hiroyoshi Nagai, Shigeki Shimizu, and Toshiichi Aota, "Fundamental Studies on Electron Beam Welding of Heat-resistant Superalloys for Nuclear Plants-Effect of Welding Conditions on Some Characteristics of Weld Bead-" Trans. of JWRI, Vol. 5 (1976), No. 2, p. 119~126.

2) D. S. Duvall and W. A. Owczarski, "Further Heat-Affected-Zone Studies on Heat-Resistant Nickel Alloys" Welding Journal, Vol. 46 (1967), No. 9, p. 423s~432s.

3) J. C. Borland, "Generalized Theory of Super-Solidus Cracking in Welds (and Casting)", British Welding Journal, Vol. 7 (1960), No. 8, p. 508~512.

4) Tomio Senda, Fukuhisa Matsuda et al., "Fundamental Investigations on Solidification Crack Susceptibility for Weld Metals with Trans-Varestraint Test" Trans. of J.W.S., Vol. 2 (1971), No. 2, p. 45~66.